

C

Contact Mechanics¹

The theory developed by Hertz in 1880 remains the foundation for most contact problems encountered in engineering. It applies to normal contact between two elastic solids that are smooth and can be described locally with orthogonal radii of curvature such as a toroid. Further, the size of the actual contact area must be small compared to the dimensions of each body and to the radii of curvature. Hertz made the assumption based on observations that the contact area is elliptical in shape for such three-dimensional bodies. The equations simplify when the contact area is circular such as with spheres in contact. At extremely elliptical contact, the contact area is assumed to have constant width over the length of contact such as between parallel cylinders. The first three sections present the Hertz equations for these distinct cases. In addition, Section C.4 presents the equations for a sphere contacting a conical socket. Hertz theory does not account for tangential forces that may develop in applications where the surfaces slide or carry traction. Extensions to Hertz theory approximate this behavior to reasonable accuracy. Section C.5 presents the more useful equations. The final section C.6 contains Mathcad™ documents that implement these equations for computer analysis.

The Hertz equations are important in the engineering of kinematic couplings particularly if the loads carried are relatively high. For a particular choice of material and contact geometry, the pertinent calculations reduce to families of curves that are convenient for sizing purposes. The typical material used is hardened bearing steel, for example, 52100 steel or 440C stainless steel heat treated to 58-62 Rockwell C. A typical contact geometry consists of a sphere against a cylindrical groove, for example, one side of a gothic arch. The graphs that follow use the elastic properties for steel and are scaled relative to the radius of the ball R_{ball} rather than its diameter. Figure C-1 shows the relationship between the load P and the maximum shear stress τ that occurs just below the surface. The allowable shear strength is approximately 58% the allowable tensile strength with $\tau = 150$ ksi being reasonable for the steels mentioned. The curves show the positive effect of curvature matching indicated by the ratio of ball radius to groove radius approaching one. A ratio of zero indicates that the groove radius is flat with infinite radius. Figure C-2 shows the normal displacement δ versus P and Figure C-3 shows the normal stiffness k versus P .

Greater load capacity and stiffness are possible by spreading the load along a line of contact, for example, with a sphere and conical socket. Three spheres and three sockets with either the spheres or the sockets supported on radial-motion blade flexures duplicate the kinematics of a three-vee coupling. The graphs that follow use the elastic properties for steel and the optimal cone angle of 45° with respect to the centerline. Figure C-4 shows the

¹ The principal reference for this chapter is Contact Mechanics by [Johnson, 1985].

relationship between the axial load P and the shear stress τ that occurs just below the surface of the contact circle. Figure C-5 shows the axial displacement δ versus P and Figure C-6 shows the axial stiffness k versus P .

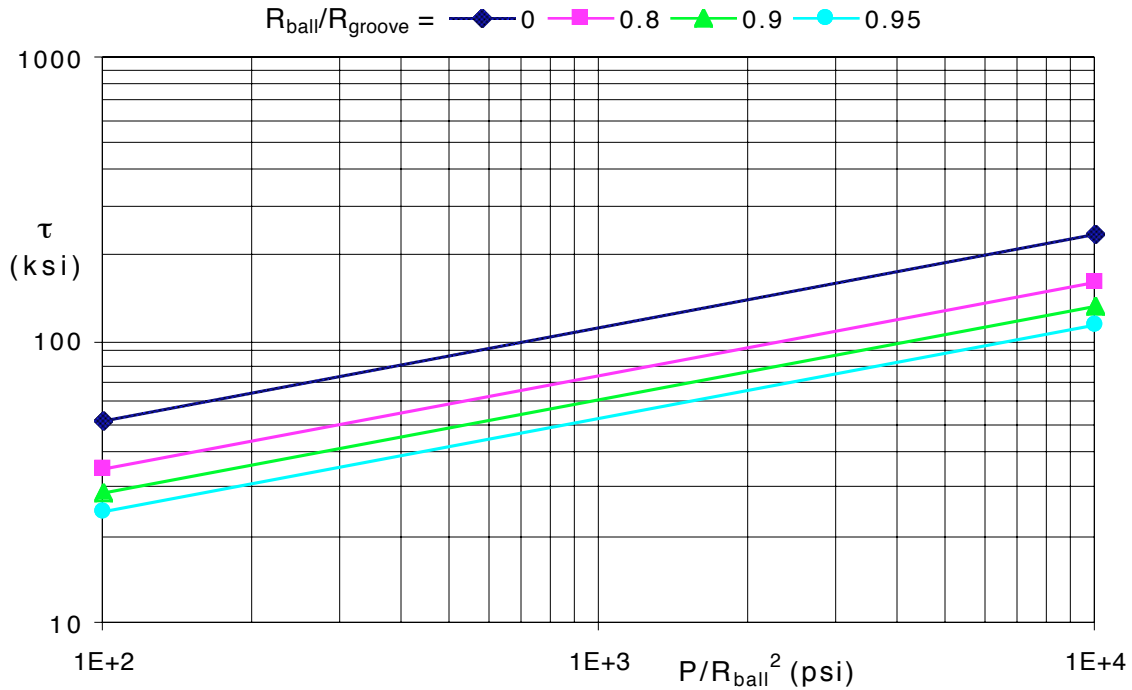


Figure C-1 Shear stress τ versus the load P for a ball against a cylindrical groove. Use this graph to determine τ , P or R_{ball} from the other two.

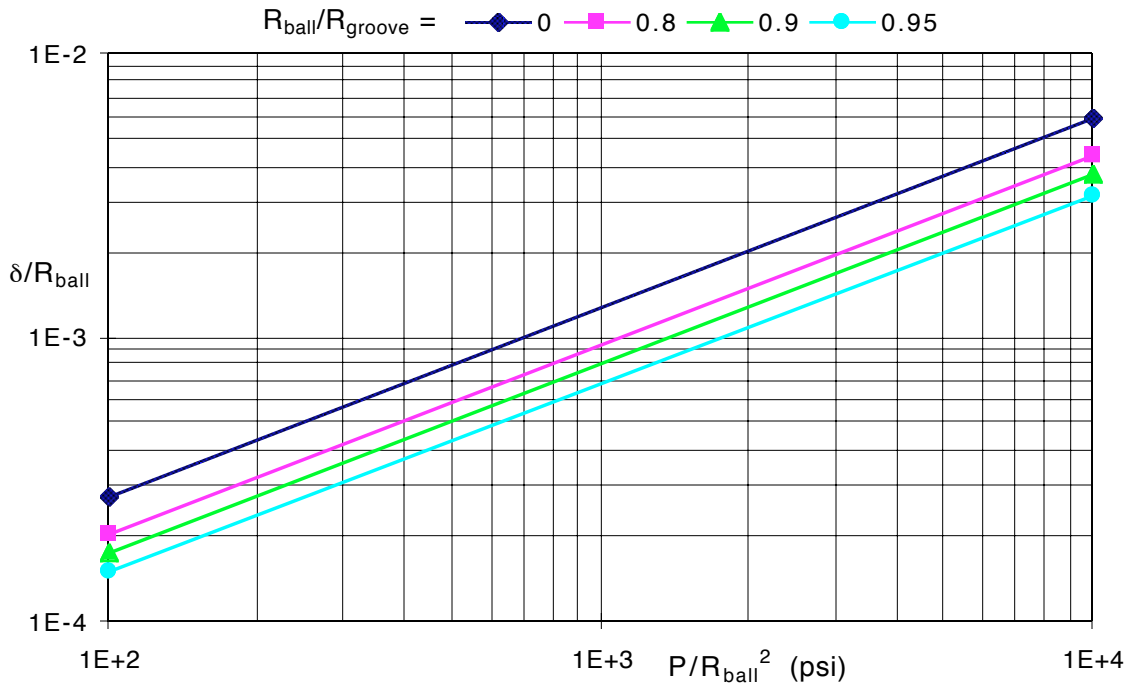


Figure C-2 Normal displacement δ versus the load P for a ball against a cylindrical groove.

Appendix C: Contact Mechanics

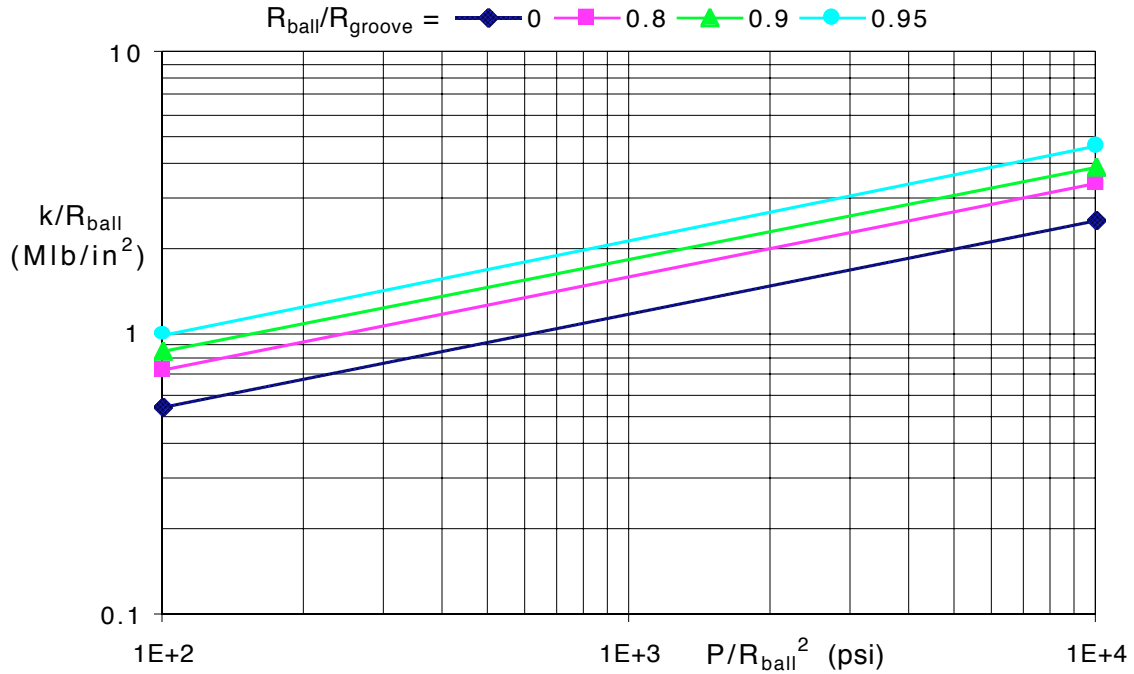


Figure C-3 Normal stiffness k versus the load P for a ball against a cylindrical groove.

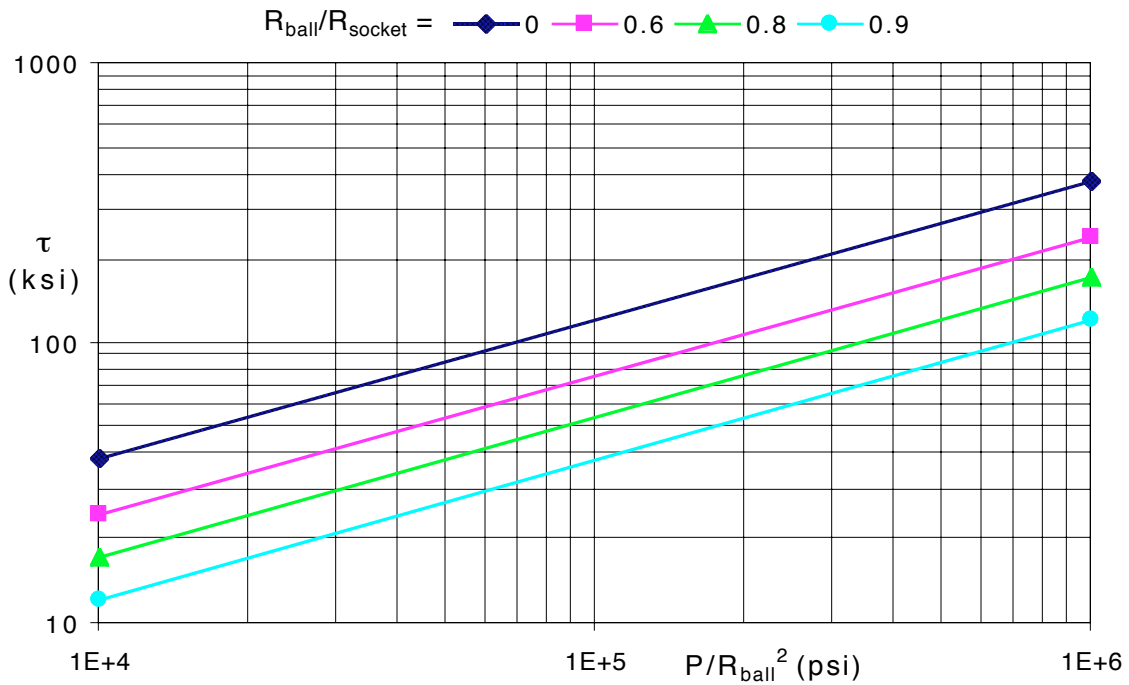


Figure C-4 Shear stress τ versus the axial load P for a ball in a conical socket. Use this graph to determine τ , P or R_{ball} from the other two.

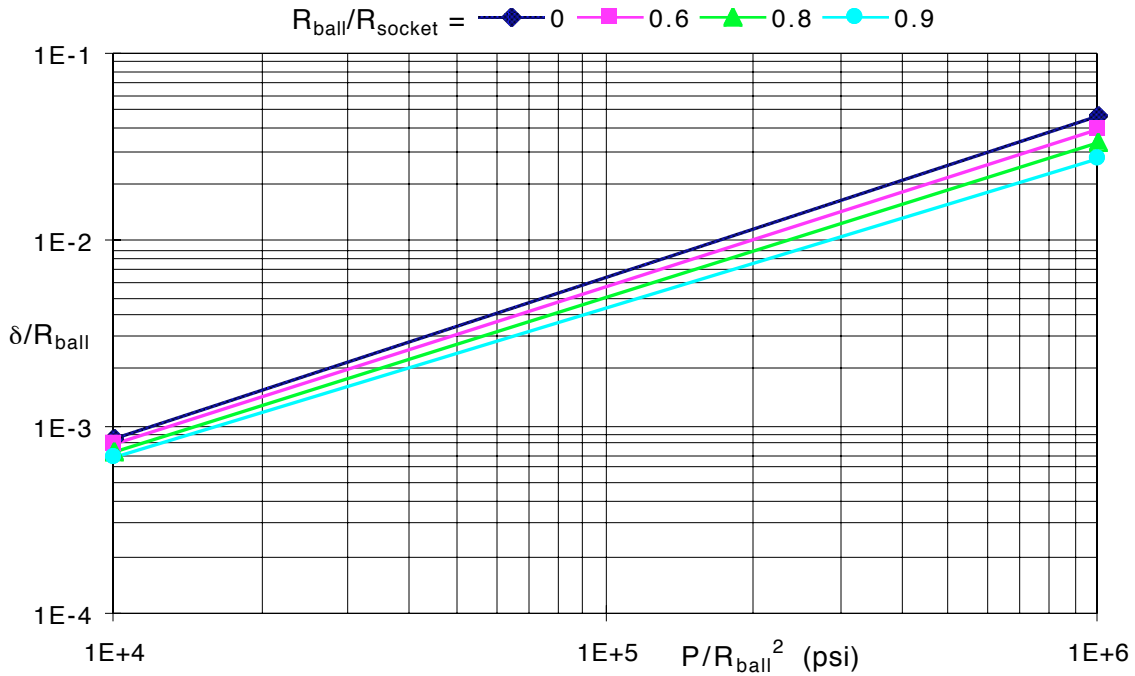


Figure C-5 Axial displacement δ versus the axial load P for a ball in a conical socket.

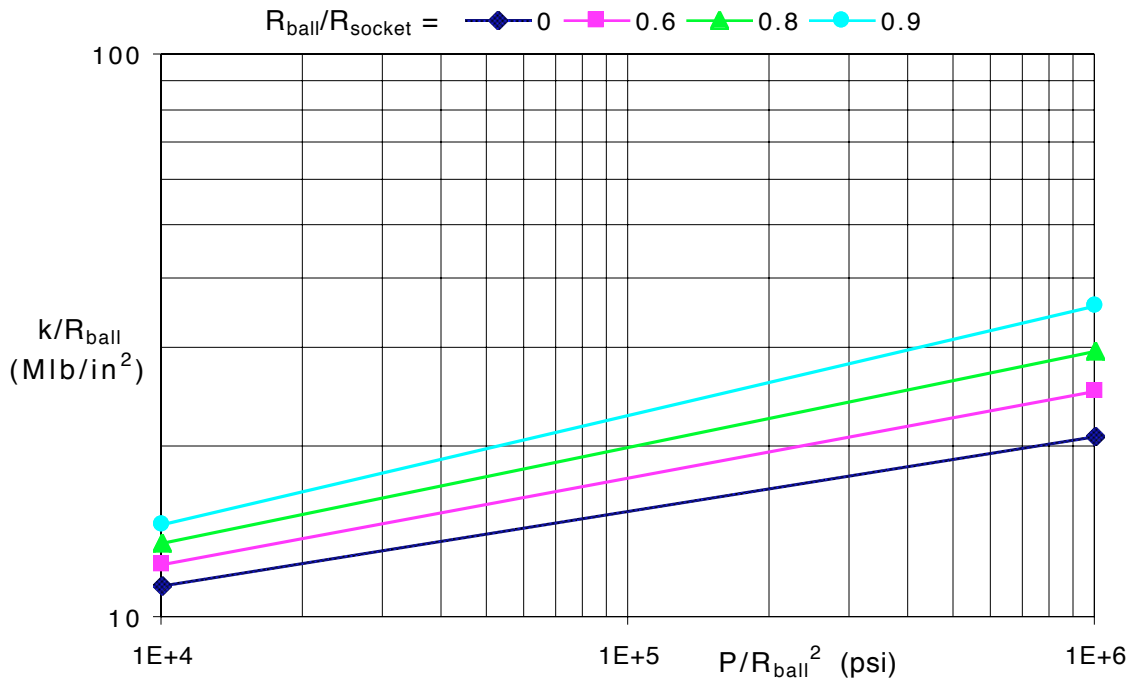


Figure C-6 Axial stiffness k versus the axial load P for a ball in a conical socket.

Applications with unusual geometry or with materials that deviate significantly from the elastic properties of steel will require analysis using the appropriate Hertz equations directly. This is not difficult given the explanations that follow and the Mathcad™ documents that implement these equations for computer analysis.

C.1 Circular Contact

A circular contact area forms when two spheres come into contact or when two cylinders of equal radius contact with 90° crossed axes. Both are special cases of elliptical contact where symmetry simplifies the equations. It is instructive to consider circular contact first to present the main concepts without undo complication.

Equations C.1 through C.8 are the Hertz equations for circular contact. The contact modulus (C.1) expresses the elastic properties of both bodies 1 and 2 effectively as a series combination of springs since stiffness is proportional to the elastic modulus for plain strain. The relative radius (C.2) expresses a summation of curvatures (or inverse radii). Note that curvature is positive for a convex surface and negative for a concave surface. Either radius may be positive or negative so long as the relative radius is positive since it represents an equivalent sphere in contact with a plane. Quite different sets of contacting surfaces behave identically if they have identical contact moduli and relative radii.

$$\text{Contact Modulus} \quad \frac{1}{E_c} = \frac{1 - \nu_1^2}{E_1} + \frac{1 - \nu_2^2}{E_2} \quad (\text{C.1})$$

$$\text{Relative Radius} \quad \frac{1}{R_c} = \frac{1}{R_1} + \frac{1}{R_2} \quad (\text{C.2})$$

The size of the circular contact (C.3) increases weakly with increasing load P and relative radius but decreases weakly with increasing contact modulus. The maximum pressure (C.4) is 1.5 times the mean pressure and occurs at the center of the contact area. Both surfaces experience the same pressure profile, which is hemispherical going to zero of course at $r = c$. Due to hydrostatic stress in the contact region, materials can endure substantially higher pressure than their tensile yield strength. Ductile materials first yield at the point of maximum shear stress (C.5) just below the surface. The allowable shear strength is approximately 58% the allowable tensile strength. Brittle materials fail by fracture at the edge of the contact where the tensile stress is maximum (C.6).

$$\text{Radius of Contact Circle} \quad c = \left(\frac{3PR_c}{4E_c} \right)^{\frac{1}{3}} \quad (\text{C.3})$$

$$\text{Maximum Pressure} \quad p = \frac{3P}{2\pi c^2} = \frac{1}{\pi} \left(\frac{6PE_c^2}{R_c^2} \right)^{\frac{1}{3}} \quad (\text{C.4})$$

$$\text{Maximum Shear Stress} \quad \tau = 0.31p \quad \text{at} \quad z = 0.48c \quad (\text{C.5})$$

$$\text{Maximum Tensile Stress} \quad \sigma = \frac{p}{3}(1 - 2\nu) \quad \text{at} \quad r = c \quad (\text{C.6})$$

The normal displacement (C.7) refers to the approach of distant points on the two bodies due primarily to deflection in the region of contact. It is obtained by integrating strain from the contact point to distant points in the bodies. The strain goes rapidly to zero thus allowing an improper integral to be bounded. The normal stiffness (C.8) is obtained by differentiating the deflection with respect to load to get compliance, then inverting.

$$\text{Normal Displacement} \quad \delta = \frac{c^2}{R_c} = \left(\frac{3P}{4E_c} \right)^{\frac{2}{3}} \left(\frac{1}{R_c} \right)^{\frac{1}{3}} \quad (\text{C.7})$$

$$\text{Normal Stiffness} \quad k = 2E_c c = \left(6PR_c E_c^2 \right)^{\frac{1}{3}} \quad (\text{C.8})$$

C.2 Elliptical Contact

An elliptical contact area forms when two three-dimensional bodies, each described locally with orthogonal radii of curvature, come into contact. In addition, the orthogonal coordinate system of one body may be rotated relative to the other by an arbitrary angle α . Any radius may be positive (convex) or negative (concave) so long as all three relative radii (C.9) are positive. To first order, R_c represents an equivalent sphere in contact with a plane, while R_a and R_b represent an equivalent toroid in contact with a plane. The contact modulus remains unchanged from circular contact (C.1). Quite different sets of contacting surfaces behave identically if they have identical contact moduli and relative radii.

$$\text{Relative Radii} \quad R_c = \sqrt{R_a R_b} \quad (\text{C.9})$$

$$R_a = \frac{1}{(A+B) - (B-A)} \quad R_b = \frac{1}{(A+B) + (B-A)}$$

$$A+B = \frac{1}{2} \left(\frac{1}{R_{1xx}} + \frac{1}{R_{1yy}} + \frac{1}{R_{2xx}} + \frac{1}{R_{2yy}} \right)$$

$$B-A = \frac{1}{2} \left\{ \left(\frac{1}{R_{1xx}} - \frac{1}{R_{1yy}} \right)^2 + \left(\frac{1}{R_{2xx}} - \frac{1}{R_{2yy}} \right)^2 \dots \right.$$

$$\left. + 2 \left(\frac{1}{R_{1xx}} - \frac{1}{R_{1yy}} \right) \left(\frac{1}{R_{2xx}} - \frac{1}{R_{2yy}} \right) \cos(2\alpha) \right\}^{\frac{1}{2}}$$

The approximate expression for the eccentricity of the contact ellipse (C.10) is sufficient for practical geometries; however, the full solution is implemented in Section C.6. The radius of an equivalent circular contact (C.11) contains a correction factor F_1 that gradually decreases from one as the contact becomes more elliptical. The major and minor

Appendix C: Contact Mechanics

radii of the contact ellipse (C.12) follow from the eccentricity and the equivalent radius. The maximum pressure (C.13) differs from circular contact only in that the pressure profile is semiellipsoidal going to zero of course at the edge of the contact ellipse. The maximum shear stress and depth below the surface (C.14) are very similar to circular contact. The equations provided are curve fits to Table 4.1 in [Johnson, 1985]. The radially oriented tensile stress at the major and minor contact radii (C.15) becomes increasingly different from one another (and the tensile stress for circular contact) as the contact becomes more elliptical. The tensile stress at the major radius σ_a is maximum.

$$\text{Eccentricity of Contact Ellipse} \quad e^2 = 1 - \left(\frac{b}{a}\right)^2 \cong 1 - \left(\frac{R_b}{R_a}\right)^{\frac{4}{3}} \quad (\text{C.10})$$

$$\text{Equivalent Radius of Contact} \quad c = \sqrt{ab} = \left(\frac{3PR_c}{4E_c}\right)^{\frac{1}{3}} F_1 \quad (\text{C.11})$$

$$\text{Major and Minor Contact Radii} \quad a = c(1 - e^2)^{-1/4} \quad b = c(1 - e^2)^{1/4} \quad (\text{C.12})$$

$$\text{Maximum Pressure} \quad p = \frac{3P}{2\pi c^2} = \frac{3P}{2\pi ab} \quad (\text{C.13})$$

$$\text{Maximum Shear Stress} \quad \tau \cong p \left\{ 0.303 + 0.0855 \frac{b}{a} - 0.808 \left(\frac{b}{a}\right)^2 \right\} \quad (\text{C.14})$$

$$z \cong b \left\{ 0.7929 - 0.3207 \frac{b}{a} \right\}$$

$$\text{Tensile Stress at } a \text{ and } b \quad \sigma_a = p(1 - 2\nu) \frac{b}{ae^2} \left\{ \frac{1}{e} \tanh^{-1}(e) - 1 \right\} \quad (\text{C.15})$$

$$\sigma_b = p(1 - 2\nu) \frac{b}{ae^2} \left\{ 1 - \frac{b}{ae^2} \tan^{-1}\left(\frac{ea}{b}\right) \right\}$$

The normal displacement (C.16) and the normal stiffness (C.17) differ from circular contact only by the correction factors F_1 and F_2 . Equation C.18 provides curve fits to the exact values as calculated in Section C.6.

$$\text{Normal Displacement} \quad \delta = \frac{c^2}{R_c} \frac{F_2}{F_1^2} = \frac{ab}{R_c} \frac{F_2}{F_1^2} \quad (\text{C.16})$$

$$\text{Normal Stiffness} \quad k = \frac{2E_c c}{F_1 F_2} \quad (\text{C.17})$$

$$F_1 \cong 1 - \left[\left(\frac{R_a}{R_b} \right)^{0.0602} - 1 \right]^{1.456} \quad F_2 \cong 1 - \left[\left(\frac{R_a}{R_b} \right)^{0.0684} - 1 \right]^{1.531} \quad (\text{C.18})$$

C.3 Line Contact

The contact between parallel cylinders away from end effects is well represented by two-dimensional Hertz theory. Then the contact area is assumed to have constant width $2b$ over the length of contact $2a$. These symbols are chosen to be consistent with elliptical contact; however to be consistent with the references, P is the line load (load per length of contact) rather than the actual load. The contact modulus (C.1) and the relative radius (C.2) remain the same as circular contact. The remaining Hertz equations for line contact are similar to but somewhat different from those of elliptical contact. The half width of contact (C.19) varies faster with load, $1/2$ versus $1/3$, but the contact area varies slower with load, $1/2$ versus $2/3$. The maximum pressure (C.20) is somewhat closer to the mean pressure, $4/\pi$ versus $3/2$. The maximum shear stress (C.21) is nearly the same ratio to the maximum pressure but occurs deeper. There is no tensile stress for line contact.

$$\text{Half Width of Contact} \quad b = \left(\frac{4PR_c}{\pi E_c} \right)^{\frac{1}{2}} \quad (\text{C.19})$$

$$\text{Maximum Pressure} \quad p = \frac{2P}{\pi b} = \left(\frac{PE_c}{\pi R_c} \right)^{\frac{1}{2}} \quad (\text{C.20})$$

$$\text{Maximum Shear Stress} \quad \tau = 0.30 p \quad \text{at} \quad z = 0.78 b \quad (\text{C.21})$$

The normal displacement (C.22) and the normal stiffness (C.23) now depend on the distance that the reference points d_1 and d_2 are from the contact point. This occurs because two-dimensional theory only allows the load to spread out in one direction. These expressions are approximate if the elastic properties are different between the two bodies; however, the exact expressions are implemented in Section C.6.

$$\text{Normal Displacement} \quad \delta \cong \frac{P}{\pi E_c} \left\{ \ln \left(\frac{4d_1}{b} \right) + \ln \left(\frac{4d_2}{b} \right) - 1 \right\} \quad (\text{C.22})$$

$$\text{Normal Stiffness} \quad k \cong \frac{\pi E_c 2a}{\ln \left(\frac{4d_1}{b} \right) + \ln \left(\frac{4d_2}{b} \right) - 2} \quad (\text{C.23})$$

C.4 Sphere and Cone Contact

The theoretical contact between a sphere and a conical socket forms a circle whose radius depends on the radius of the sphere R and the cone angle θ with respect to the axis. Hertz theory for line contact may be extended to sphere and cone contact rather simply by assuming the line load (C.24) consists of a constant term due to the axial load f_a and a sinusoidal variation around the circle due to the radial load f_r . The maximum and minimum line loads occur at $\phi = 0$ and π radians, respectively. Then maximum and minimum values of contact width, pressure and so forth are simple to calculate using the Hertz equations for line contact. The axial stiffness (C.25) and the radial stiffness (C.26) come from integrating the local contact stiffness (reflected to the proper angle) around the circle. Since the local contact stiffness does not usually change significantly around the circle, it is adequate to use the mean value to simplify the integration.

$$\text{Line Load} \quad P(\theta, \phi) \cong \frac{1}{2\pi R \cos(\theta)} \left\{ \frac{f_a}{\sin(\theta)} + \frac{2 \cos(\phi) f_r}{\cos(\theta)} \right\} \quad (\text{C.24})$$

$$\text{Axial Stiffness} \quad k_a \cong \frac{2\pi^2 E_c R \cos(\theta) \sin^2(\theta)}{\ln\left(\frac{4d_1}{b_{\max}}\right) + \ln\left(\frac{4d_2}{b_{\min}}\right) - 2} \quad (\text{C.25})$$

$$\text{Radial Stiffness} \quad k_r \cong \frac{\pi^2 E_c R \cos^3(\theta)}{\ln\left(\frac{4d_1}{b_{\max}}\right) + \ln\left(\frac{4d_2}{b_{\min}}\right) - 2} \quad (\text{C.26})$$

C.5 Tangential Loading of an Elliptical Contact

The normal pressure that exists between two three-dimensional bodies in contact has a semiellipsoidal profile that is maximum at the center and zero at the boundary of the contact area. It is reasonable to expect the same profile to exist for surface traction if the two bodies also slide while held in contact. The traction in this case is related to the normal pressure through the coefficient of friction. If it were possible to perfectly adhere the surfaces in some way, then a tangential force would cause the reciprocal profile to develop over the contact. In this case the traction is minimum at the center and rises to infinity along the edge. This is plausible behavior since the joint is equivalent to a very deep, sharp crack. The friction connection obviously cannot support infinite traction where the normal force is zero. A region of slip forms at the edge of contact and extends toward the center until the

normal pressure is sufficient to carry the traction by friction.^I As the tangential force increases, the slip region encroaches further into the adhered region until nothing remains to prevent sliding, and the tangential stiffness goes to zero. The useful tangential constraint device typically operates well below the point of incipient sliding.

This theory has practical applications in the design of friction drives for precision machines and also in kinematic couplings where frictional constraints act to stiffen the coupling and the flexible modes of the supported object. Slip between two elastic bodies is a dynamic process that requires something to change. This section treats the two most practical possibilities: when the contact is stationary and the tangential force varies, or when the force is constant and the contact moves across rolling bodies.^{II} For example, slip that occurs from an oscillating tangential force results in a hysteresis loop in the force-displacement curve. Slip that occurs between rolling bodies in contact results in a small differential velocity called creep in the literature. These nonideal behaviors are usually very small and can be estimated with reasonable accuracy using the equations provided.

C.5.1 Stationary Elliptical Contact, Variable Tangential Force

A tangential force applied to a stationary, elliptical contact produces a relative tangential displacement governed principally by elastic deformation in the contact. Typically small inelastic behavior results from slip that always accompanies the elastic deformation. In the normal direction, all the Hertz equations for elliptical contact still apply. Since traction at the surface produces shear stress in the material, it is convenient to define the contact shear modulus (C.27) to simplify the main equations. The transition from an adhered region to a slip region occurs theoretically on an ellipse that is smaller in size but with the same proportions as the contact ellipse. The transition ellipse (C.28) shrinks in size as the tangential force increases until the point of incipient sliding occurs when $T = \mu P$. The subscript in the equation indicates that the traction profile may have more than one transition depending on the history of the tangential force. The tangential displacement between distant points (C.29) is valid when there is one transition in the traction profile. This occurs if the contact initially has zero traction and the tangential force increases monotonically. Corresponding to this condition is the tangential stiffness (C.30), which applies only when the force increases. A decreasing force causes the entire contact to momentarily adhere then establish a second transition ellipse outside the first.

$$\text{Contact Shear Modulus} \quad \frac{1}{G_c} = \frac{2 - \nu_1}{G_1} + \frac{2 - \nu_2}{G_2} \quad (\text{C.27})$$

^I It is customary to distinguish between the terms *slip* and *sliding*. Slip refers to small relative displacement resulting from differing strain fields in the two contacting surfaces. Sliding is arbitrarily large movement between two contacting surfaces.

^{II} [Mindlin and Deresiewicz, 1953] treat combinations of varying normal and tangential force.

Appendix C: Contact Mechanics

$$\text{Transition Ellipse} \quad \frac{a_1}{a} = \frac{b_1}{b} = \left(1 - \frac{T_1}{\mu P}\right)^{\frac{1}{3}} \quad (\text{C.28})$$

$$\text{Tangential Displacement} \quad \delta = \frac{3 \mu P}{16 a G_c} \left\{ 1 - \left(1 - \frac{T}{\mu P}\right)^{\frac{2}{3}} \right\} \Phi \quad (\text{C.29})$$

$$\text{Tangential Stiffness} \quad k = 8 a G_c \left(1 - \frac{T}{\mu P}\right)^{\frac{1}{3}} \frac{1}{\Phi} \quad (\text{C.30})$$

The equation for the second transition ellipse (C.31) depends on the maximum tangential force T_1 and the relaxed or reversed tangential force T_2 . If the magnitude of T_2 becomes equal to or greater than T_1 , then the second transition ellipse encroaches on the first and effectively eliminates its record. It is possible in theory to have several transitions if there are several reversals and each is smaller than the previous one. The tangential displacement for a decreasing tangential force (C.32) has an added term to account for the second transition. Setting T to zero gives the half width of the hysteresis loop between $\pm T_1$. An approximate expression of the hysteresis half width (C.33) is primarily quadratic in T_1 . The tangential stiffness for a decreasing tangential force (C.34) is momentarily maximum, as expected, then it decreases as the tangential force relaxes. Notice that all the equations for displacement and stiffness share the correction factor Φ . This factor accounts for the ellipticity of the contact and whether the tangential force is parallel to the major radius a or the minor radius b . The approximate correction factor (C.35) provides good agreement with the more complicated exact expressions plotted in Figure C-7. The exact expressions are used in Section C.6.

$$\text{Transition Ellipse} \quad \frac{a_2}{a} = \frac{b_2}{b} = \left(1 - \frac{T_1 - T_2}{2\mu P}\right)^{\frac{1}{3}} \quad (\text{C.31})$$

$$\text{Tangential Displacement} \quad \delta_d = \frac{3 \mu P}{16 a G_c} \left\{ 2 \left(1 - \frac{T_1 - T}{2\mu P}\right)^{\frac{2}{3}} - \left(1 - \frac{T_1}{\mu P}\right)^{\frac{2}{3}} - 1 \right\} \Phi \quad (\text{C.32})$$

$$\text{Hysteresis Half Width} \quad \delta_h \cong \frac{3 \mu P}{16 a G_c} \left\{ \frac{1}{18} \left(\frac{T_1}{\mu P}\right)^2 + \frac{1}{27} \left(\frac{T_1}{\mu P}\right)^3 \right\} \Phi \quad (\text{C.33})$$

$$\text{Tangential Stiffness} \quad k_d = 8 a G_c \left(1 - \frac{T_1 - T}{2\mu P}\right)^{\frac{1}{3}} \frac{1}{\Phi} \quad (\text{C.34})$$

Correction Factor $\Phi \cong \begin{cases} 1 + (1.4 - 0.8\nu)\log\left(\frac{a}{b}\right) & T // b \\ 1 & a = b \\ 1 + (1.4 + 0.8\nu)\log\left(\frac{a}{b}\right) & T // a \end{cases} \quad (C.35)$

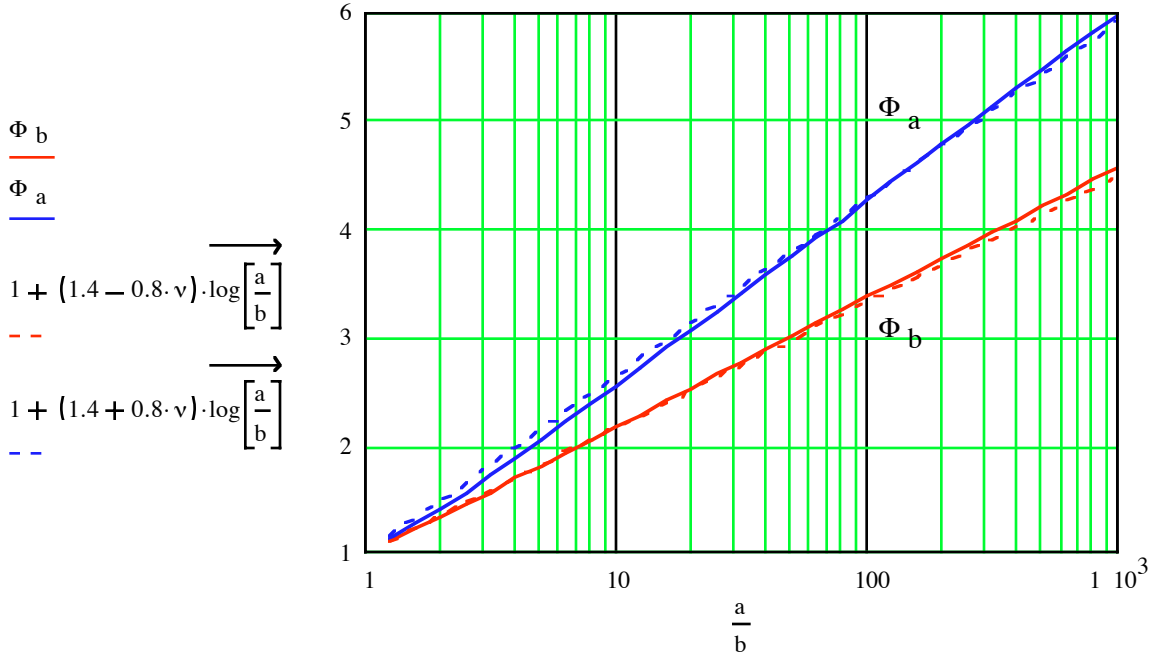


Figure C-7 Correction factors for elliptical contact calculated for $\nu = 0.3$. The tangential force may be parallel with the major radius a or the minor radius b .

The following references present this theory in greater detail [Mindlin, 1949], [Mindlin and Deresiewicz, 1953], [Deresiewicz, 1957]. One reference [Mindlin, et al., 1951] provides experimental data that agrees reasonably well with theory except for the energy dissipation for low-amplitude cycles. The theory predicts that the energy loss is cubic in force amplitude whereas the experiment shows quadratic behavior.

C.5.2 Rolling Circular Contact, Constant Tangential Force

The equations for slip in a rolling circular contact due to a constant tangential force are very similar to those for stationary contact. This is understandable since the theory developed by [Johnson, 1958] assumes that the transition between the adhered region and the slip region is the same proportion described in Equation C.28. He further assumes that the adhered region is tangent to the leading edge of contact whether the tangential force is parallel to or perpendicular to the direction of travel. This is intuitive behavior since the material entering the contact area is in a relaxed state and acquires increasing traction until it exceeds the threshold for slip towards the trailing edge of contact. A numerical approach developed by [Kalker, 1966] predicts a lemon-shaped adhered region bounded by the leading edge of the

Appendix C: Contact Mechanics

contact circle and an arc shifted from the trailing edge. The slip region then appears as a crescent. Although the numerical approach closely matches observed results, Johnson's theory yields simple equations and reasonable estimates of creep (the ratio of the slip velocity to the rolling-contact velocity).

The direction of the tangential force governs the direction of slip but it plays a minor role in the magnitude of the slip ratio. Johnson uses the term *longitudinal* to indicate that the tangential force is in the direction of rolling along the x -axis. A *transverse* tangential force is in the y -direction. As before, it is convenient to group the elastic properties of both bodies into one. The longitudinal and transverse shear moduli (C.36 and C.37) differ only about ± 10 percent from the contact shear modulus (C.27). Given the approximate nature of this theory, it would be adequate to use the contact shear modulus (C.27) for any direction of tangential force. Other than accounting for differences in directions, the longitudinal and transverse slip ratios (C.38 and C.39) are identical.

$$\text{Longitudinal Shear Modulus} \quad \frac{1}{G_x} = \frac{2 - 1.5\nu_1}{G_1} + \frac{2 - 1.5\nu_2}{G_2} \quad (\text{C.36})$$

$$\text{Transverse Shear Modulus} \quad \frac{1}{G_y} = \frac{2 - 0.5\nu_1}{G_1} + \frac{2 - 0.5\nu_2}{G_2} \quad (\text{C.37})$$

$$\text{Longitudinal Slip Ratio} \quad \xi_x = \frac{3 \mu P}{16 c^2 G_x} \left\{ 1 - \left(1 - \frac{T_x}{\mu P} \right)^{\frac{1}{3}} \right\} \quad (\text{C.38})$$

$$\text{Transverse Slip Ratio} \quad \xi_y = \frac{3 \mu P}{16 c^2 G_y} \left\{ 1 - \left(1 - \frac{T_y}{\mu P} \right)^{\frac{1}{3}} \right\} \quad (\text{C.39})$$

Although this theory was developed for circular contact, its similarity to stationary contact suggests that it could be extended to elliptical contact using the same correction factor Φ . The use of Φ_a or Φ_b and particularly whether to use $c^2 = a b$ or a^2 in the denominator is strictly conjecture. The recommendation is to use $a b$ when rolling is along the minor axis, and conversely to use a^2 when rolling is along the major axis. The rationale is that one factor of a belongs with Φ and that the slip ratio scales inversely with the contact width in the direction of rolling, either a or b . The choice of Φ_a or Φ_b depends solely on whether the tangential force is along the major or minor axis. The use of longitudinal or transverse shear modulus is optional.

Experimental work by [Johnson, 1958] shows reasonable agreement with his theory for rolling contact of a sphere on a plane. The agreement is good for low levels of slip but it underestimates creep by 20 to 30 percent for $T > \mu P/2$.